

Supporting information

Charge, Adsorption, Water Stability and Bandgap Tuning of An Anionic Cd(II) Porphyrinic Metal-Organic Framework

Qi Li,^a Yanping Luo,^{ad} Yue Ding,^a Yina Wang,^a Yuxin Wang,^a Hongbin Du,^b Rongxin Yuan,^c Jianchun Bao,^d Min Fang,^{*ab} Yong Wu^{*a}

- ^a. Jiangsu Key Laboratory of New Power Batteries, Jiangsu Collaborative Innovation Center of Biomedical Functional Materials, School of Chemistry and Materials Science, Nanjing Normal University, Nanjing 210023, PR China. Email: fangmin@njnu.edu.cn, wuyong@njnu.edu.cn
- ^b. State Key Laboratory of Coordination Chemistry, Nanjing University, Nanjing 210093, China
- ^c. School of Chemistry and Materials Engineering, Changshu Institute of Technology, Changshu, 215500, China.
- ^d. Jiangsu Key Laboratory of Biofunctional Materials, School of Chemistry and Materials Science, Nanjing Normal University, Nanjing 210023, China.

* Corresponding authors.

Keywords: Anionic MOF, metal porphyrinic framework, band edge position, band gap tuning, visible light, CO₂ reduction

Contents

Table S1 Crystallographic data for 1 and 1(6:1)-2d.	3
Table S2 Selected bond distances (Å) and angles (degrees) for 1.	4
Table S3 Selected bond distances (Å) and angles (degrees) for 1(6:1)-2d.	6
Topology analysis of compound 1.	8
Fig. S1 4,4,8-c underlying net (nnu3) of compound 1.	8
Fig. S2 The rod packing structure of compound 1.	8
Fig. S3 The 2-nodal 4,6-coordinated 4,6T156 topology of compound 1.	9
IR spectra.	10
Fig. S4 IR spectra of 1-DMF, 1-ex, 1(4:1)-4d-DMF, 1(6:1)-4d-DMF, and 1(8:1)-4d-DMF (a); IR spectra of Li ⁺ -1-2d, Li ⁺ -1-5d, and Li ⁺ -1-10d (b); IR and Raman spectra of H ₆ TCPD compared with IR spectra of 1-ex and 1(8:1)-4d-DMF (c).	10
Fig. S5 TG/DTA of 1-ex (a) 1(4:1)-4d-ex (b) and 1(8:1)-4d-ex (c), Li ⁺ -1-2d (d), Li ⁺ -1-5d (e), and Li ⁺ -1-10d.	Error! Bookmark not defined.
Fig. S6 PXRD spectrum of 1-DMF after two cycles of photocatalytic CO ₂ reduction.	12
Fig. S7 CO ₂ (273 and 298 K) and CH ₄ (273 and 298 K) adsorption/desorption isotherms of 1(4:1)-4d-ex (a), 1(6:1)-4d-ex (b), and 1(8:1)-4d-ex (c).	13
Fig. S8 CO ₂ (273 and 298 K) and CH ₄ (273 and 298 K) adsorption/desorption isotherms of Li ⁺ -1-5d (a) and Li ⁺ -1-10d (b).	13
Fig. S9 Band gaps of 1(4:1)-4d-ex, 1(6:1)-4d-ex, 1(8:1)-4d-ex, Li ⁺ -1-2d, Li ⁺ -1-5d, and Li ⁺ -1-10d determined by plots of (<i>abs</i> or [<i>abs</i> (<i>hν</i>)] ^{1/2} or [<i>abs</i> (<i>hν</i>)] ² versus <i>hν</i>	14
Fig. S10 Cathodic and anodic linear potential scans for determining the positions of the CB and VB edges of 1-DMF, 1-ex, and 1(8:1)-2d-DMF using pH=5.34 H ₂ SO ₄ aqueous solution or the Tris-HCl buffered saline solution (0.1 mol L ⁻¹ , pH 7.4).	15
Fig. S11 Cathodic and anodic linear potential scans for determining the positions of the CB and VB edges of 1(4:1)-4d-ex ((a)-(d)), 1(6:1)-4d-ex ((e)-(h)) and 1(8:1)-4d-ex ((i)-(l)) using two different electrolytes (the pH 5.01 H ₂ SO ₄ aqueous solution or the Tris-HCl buffered saline solution (0.1 mol·L ⁻¹ , pH 7.4)).	16
Fig. S12 Cathodic and anodic linear potential scans for determining the positions of the CB and VB edges of Li ⁺ -1-2d ((a)-(d)), Li ⁺ -1-5d ((e)-(h)) and Li ⁺ -1-10d ((i)-(l)) using two different electrolytes (the pH 5.01 H ₂ SO ₄ aqueous solution or the Tris-HCl buffered saline solution (0.1 mol L ⁻¹ , pH 7.4)).	18

Table S1 Crystallographic data for 1 and 1(6:1)-2d.

Compound	1	1(6:1)-2d
Formula	C _{114.20} H _{98.80} Cd _{3.20} N _{14.60} O _{23.50}	C _{113.76} H _{104.04} Cd _{3.31} N _{14.38} O ₂₄
<i>F</i> _w	1933.17	2408.47
Crystal system	Monoclinic	Monoclinic
Space group	<i>C</i> 2/ <i>c</i>	<i>C</i> 2/ <i>c</i>
<i>a</i> (Å)	7.089(2)	7.0923 (16)
<i>b</i> (Å)	26.513(8)	26.431(6)
<i>c</i> (Å)	30.078(8)	30.165(8)
β (°)	95.351(8)	95.216(3)
<i>V</i> (Å ³)	5628(3)	5631(2)
<i>Z</i>	2	2
<i>D</i> _c (g/cm ³)	1.423	1.420
μ (mm ⁻¹)	0.675	0.695
<i>T</i> (K)	296(2)	296(2)
Total reflections	32793	56916
Unique data collected	4906	6167
Observed reflections	3749	3210
<i>R</i> _{int}	0.063	0.142
<i>R</i> ₁ , <i>wR</i> ₂ (<i>I</i> > 2σ(<i>I</i>))	0.0951, 0.2695	0.086, 0.1761
<i>R</i> ₁ , <i>wR</i> ₂ (all data)	0.1075, 0.2837	0.1671, 0.2151
Goodness of fit on <i>F</i> ²	1.141	1.036

Table S2 Selected bond distances (Å) and angles (degrees) for 1.

C1—O2	1.24(2)	C13—C14	1.467(9)
C1—O1	1.293(16)	C1—C2	1.497(18)
C14—C15	1.3900	C14—C19	1.3900
C2—C3	1.3900	C15—C16	1.3900
C2—C7	1.3900	C15—H15	0.9300
C3—C4	1.3900	C16—C17	1.3900
C3—H3A	0.9599	C16—H16	0.9300
C4—C5	1.3900	C17—C18	1.3900
C4—H4A	0.9600	C17—C20	1.561(11)
C5—C6	1.3900	C18—C19	1.3900
C5—C8	1.477(10)	C18—H18	0.9300
C6—C7	1.3900	C19—H19	0.9300
C6—H6A	0.9601	C7—H7A	0.9600
O1—Cd2ii	2.314(8)	O1—Cd2iii	2.355(8)
O1—Cd1i	2.570(14)	O2—Cd1i	2.234(18)
C8—C24iv	1.339(12)	C8—C9	1.411(11)
C20—O4	1.247(9)	C20—O3	1.250(8)
C21—N2	1.372(9)	C21—C22	1.421(12)
C22—C23	1.343(16)	C22—H22A	0.9300
C23—C24	1.439(11)	C23—H23A	0.9300
C24—N2	1.343(10)	Cd1—O4	2.424(7)
Cd1—O4v	2.424(7)	Cd1—O3	2.521(13)
Cd1—O3v	2.521(13)	Cd2—Cd2vi	0.598(2)
C9—N1	1.373(11)	Cd2—O4vi	2.190(7)
C9—C10	1.480(13)	Cd2—O4	2.559(6)
C10—C11	1.326(15)	N2—H2A	0.8600
C10—H10A	0.9300	C11—C12	1.417(13)
C11—H11A	0.9300	C12—N1	1.365(9)
C12—C13	1.398(12)	C13—C21	1.400(13)
O2—C1—O1	124.1(17)	O2—C1—C2	116.6(12)
O1—C1—C2	119.3(16)	O2—C1—Cd1i	54.4(10)
O1—C1—Cd1i	69.8(9)	C2—C1—Cd1i	170.3(11)
C3—C2—C7	120.0	C3—C2—C1	120.1(9)
C7—C2—C1	119.8(9)	C4—C3—C2	120.0
C4—C3—H3A	120.0	O4—C20—O3	121.8(6)
C2—C3—H3A	120.0	C3—C4—C5	120.0
C3—C4—H4A	120.0	O4—C20—C17	120.1(5)
C5—C4—H4A	120.0	O3—C20—C17	117.7(6)
C6—C5—C4	120.0	C6—C5—C8	121.9(6)
C4—C5—C8	118.1(6)	C5—C6—C7	120.0
N2—C21—C13	127.7(6)	C5—C6—H6A	120.0
N2—C21—C22	107.3(9)	C7—C6—H6A	120.0
C13—C21—C22	125.0(7)	C6—C7—C2	120.0
C23—C22—C21	107.5(7)	C6—C7—H7A	120.0
C23—C22—H22A	126.3	C2—C7—H7A	120.0
C21—C22—H22A	126.3	C1—O1—Cd2ii	134.2(8)
C22—C23—C24	108.5(9)	C1—O1—Cd2iii	141.2(8)
C22—C23—H23A	125.7	Cd2ii—O1—Cd2iii	14.69(8)
C24—C23—H23A	125.7	C1—O1—Cd1i	82.1(11)
C8iv—C24—N2	125.9(7)	Cd2ii—O1—Cd1i	91.1(4)
C8iv—C24—C23	127.4(9)	Cd2iii—O1—Cd1i	104.3(4)
N2—C24—C23	106.6(8)	C1—O2—Cd1i	98.7(10)
O2vii—Cd1—O2i	77.5(10)	C24iv—C8—C9	128.6(8)
O2vii—Cd1—O4	125.0(5)	O2i—Cd1—O4	86.0(5)
C24iv—C8—C5	111.1(7)	O2vii—Cd1—O4v	86.0(4)
C9—C8—C5	120.2(9)	O4—Cd1—O4v	142.2(8)
O2i—Cd1—O4v	125.0(5)	O2i—Cd1—O3	96.5(4)

O2vii—Cd1—O3	173.9(7)	O2vii—Cd1—O1i	84.9(6)
O4—Cd1—O3	52.3(3)	O2i—Cd1—O1i	54.9(5)
C19—C14—C13	116.7(6)	C20—O4—Cd2	153.8(5)
C14—C15—C16	120.0	Cd2vi—O4—Cd2	11.43(6)
C14—C15—H15	120.0	Cd1—O4—Cd2	102.7(4)
C16—C15—H15	120.0	C17—C16—C15	120.0
C17—C16—H16	120.0	C15—C16—H16	120.0
C18—C17—C16	120.0	C18—C17—C20	117.7(5)
C16—C17—C20	121.7(5)	C19—C18—C17	120.0
C19—C18—H18	120.0	C17—C18—H18	120.0
C18—C19—C14	120.0	C18—C19—H19	120.0
C14—C19—H19	120.0	O2—C1—C2—C3	-10.0(16)
C21—C13—C14—C19	-76.8(9)	C17—C20—O4—Cd2	-44.1(19)
O1—C1—C2—C3	169.9(9)	C19—C14—C15—C16	0.0
O2—C1—C2—C7	167.5(11)	C13—C14—C15—C16	169.7(11)
O1—C1—C2—C7	-12.6(14)	C14—C15—C16—C17	0.0
C7—C2—C3—C4	0.0	C15—C16—C17—C18	0.0
C1—C2—C3—C4	177.5(9)	C15—C16—C17—C20	-171.0(10)
C2—C3—C4—C5	0.0	C16—C17—C18—C19	0.0
C3—C4—C5—C6	0.0	C20—C17—C18—C19	171.4(10)
C3—C4—C5—C8	179.0(8)	C17—C18—C19—C14	0.0
C4—C5—C6—C7	0.0	C15—C14—C19—C18	0.0
C8—C5—C6—C7	-178.9(9)	C13—C14—C19—C18	-170.3(11)
C5—C6—C7—C2	0.0	C3—C2—C7—C6	0.0
C1—C2—C7—C6	-177.5(9)	C12—C13—C14'—C19'	98.3(13)
O2—C1—O1—Cd2ii	87.5(19)	C2—C1—O1—Cd2ii	-92.4(17)
Cd1i—C1—O1—Cd2ii	83.8(13)	O2—C1—O1—Cd2iii	106.8(19)
C2—C1—O1—Cd2iii	-73(2)	Cd1i—C1—O1—Cd2iii	103.0(16)
O2—C1—O1—Cd1i	3.8(15)	C2—C1—O1—Cd1i	-176.1(11)
O1—C1—O2—Cd1i	-4.3(17)	C2—C1—O2—Cd1i	175.6(9)
C6—C5—C8—C24iv	57.8(9)	C4—C5—C8—C24iv	-121.2(7)
C6—C5—C8—C9	-118.1(9)	C4—C5—C8—C9	62.9(10)
C18—C17—C20—O4	2.1(13)	C17—C20—O4	173.3(7)
C18—C17—C20—O3	174.8(8)	C17—C20—O3	-14.0(12)
C13—C21—N2	1.9(12)	C14—C13—C21—N2	178.1(7)
C13—C21—N2	166.2(12)	C12—C13—C21—C22	-179.2(8)
C13—C21—C22	-3.0(11)	C13—C21—C22	-14.9(15)
N2—C21—C22—C23	-0.4(10)	C21—C22—C23	-179.5(8)
C21—C22—C23—C24	0.4(10)	C22—C23—C24—C8iv	-176.2(9)
C22—C23—C24—N2	-0.2(10)	C13—C12—N1—C9	175.9(7)
C11—C12—N1—C9	-2.7(9)	C8—C9—N1—C12	-175.6
C24iv—C8—C9—N1	-1.6(14)	C10—C9—N1—C12	4.5(10)
C5—C8—C9—N1	173.5(8)	C8iv—C24—N2—C21	176.0(7)
C24iv—C8—C9—C10	178.3(10)	C23—C24—N2—C21	-0.1(8)
C5—C8—C9—C10	-6.6(14)	C13—C21—N2—C24	179.4(7)
C22—C21—N2—C24	0.3(8)	N1—C9—C10—C11	-4.6(12)
C8—C9—C10—C11	175.5(10)	O4—C20—O3—Cd1	-11.3(10)
C9—C10—C11—C12	2.9(13)	C17—C20—O3—Cd1	176.1(9)
C10—C11—C12—N1	-0.2(13)	C10—C11—C12—C13	-178.8(9)
N1—C12—C13—C21	1.3(12)	O3—C20—O4—Cd2vi	124.6(8)
C11—C12—C13—C21	179.6(9)	C17—C20—O4—Cd2vi	-62.9(15)
N1—C12—C13—C14	-174.4(8)	O3—C20—O4—Cd1	11.8(10)
C11—C12—C13—C14	3.9(13)	C17—C20—O4—Cd1	-175.7(10)
C12—C13—C14—C15	-70.6(11)	C21—C13—C14—C15	113.2(7)
O3—C20—O4—Cd2	143.4(9)	C12—C13—C14—C19	99.4(9)

Symmetry codes: (i) $-x+1, -y+1, -z+1$; (ii) $-x, -y+1, -z+1$; (iii) $x-1, -y+1, z-1/2$; (iv) $-x-1/2, -y+1/2, -z+1$; (v) $-x+2, y, -z+3/2$; (vi) $-x+1, y, -z+3/2$; (vii) $x+1, -y+1, z+1/2$.

Table S3 Selected bond distances (Å) and angles (degrees) for 1(6:1)-2d.

Cd1—O2	2.344	(5)	C21B—C20B	1.41	(2)
Cd1—O2i	2.344	(5)	C13B—C14B	1.45	(3)
Cd1—O1i	2.353	(6)	C18B—C17B	1.51	(2)
Cd1—O1	2.353	(6)	C14B—H14B	0.930	
Cd1—O3Bii	2.402	(11)	C22B—H22B	0.930	
Cd1—O3Biii	2.402	(11)	C20B—H20B	0.930	
Cd1—O4Aiii	2.117	(19)	O4A—C24A	1.238	(18)
Cd1—O4Aii	2.117	(19)	O3A—C24A	1.262	(18)
Cd2—O2iv	2.375	(6)	N2A—C13A	1.31	(7)
Cd2—O2v	2.375	(6)	N2A—C16A	1.63	(9)
Cd2—O4Bvi	2.340	(8)	C13A—C14A	1.40	(7)
Cd2—O4Bvii	2.340	(8)	C21A—C22A	1.44	(4)
Cd2—O3Aviii	2.438	(18)	C21A—C24A	1.515	(18)
Cd2—O3A	2.439	(18)	C21A—C20A	1.42	(4)
O2—C1	1.245	(9)	C14A—H14A	0.930	
O1—C1	1.234	(8)	C14A—C15A	1.45	(6)
N1—H1	0.860		C19A—H19A	0.930	
N1—C12	1.355	(10)	C19A—C18A	1.43	(4)
N1—C9	1.368	(9)	C19A—C20A	1.38	(4)
C12—C11	1.450	(12)	C22A—H22A	0.930	
C12—C17Bix	1.462	(19)	C22A—C23A	1.35	(4)
C12—C17Aix	1.27	(4)	C15A—H15A	0.930	
C10—H10	0.930		C15A—C16A	1.40	(6)
C10—C11	1.362	(13)	C17A—C18A	1.51	(2)
C10—C9	1.426	(13)	C17A—C16A	1.41	(5)
C11—H11	0.930		C23A—H23A	0.930	
C9—C8	1.380	(11)	C23A—C18A	1.38	(4)
C8—C13B	1.28	(2)	C20A—H20A	0.930	
C8—C13A	1.64	(4)	C3B—H3B	0.930	
C8—C5B	1.496	(9)	C3B—C2B	1.390	
C8—C5A	1.58	(3)	C3B—C4B	1.390	
C1—C2B	1.517	(9)	C2B—C7B	1.390	
C1—C2A	1.45	(3)	C7B—H7B	0.930	
O4B—C24B	1.248	(12)	C7B—C6B	1.390	
O3B—C24B	1.225	(14)	C6B—H6B	0.930	
N2B—C16B	1.27	(4)	C6B—C5B	1.390	
N2B—C13B	1.43	(3)	C5B—C4B	1.390	
C16B—C15B	1.47	(2)	C4B—H4B	0.930	
C16B—C17B	1.37	(2)	C5A—C6A	1.390	
C19B—H19B	0.930		C5A—C4A	1.390	
C19B—C18B	1.376	(18)	C6A—H6A	0.930	
C19B—C20B	1.339	(19)	C6A—C7A	1.390	
C15B—H15B	0.930		C7A—H7A	0.930	
C15B—C14B	1.32	(3)	C7A—C2A	1.390	
C23B—H23B	0.930		C2A—C3A	1.390	
C23B—C18B	1.32	(2)	C3A—H3A	0.930	
C23B—C22B	1.39	(2)	C3A—C4A	1.390	
C21B—C24B	1.549	(19)	C4A—H4A	0.930	
C21B—C22B	1.388	(18)			
O2—Cd1—O2i	153.1	(3)			
O2i—Cd1—O1i	54.45	(18)			
O2—Cd1—O1	54.45	(18)	C23B—C18B—C19B	120.4	(15)
O2—Cd1—O1i	106.1	(2)	C23B—C18B—C17B	121.3	(14)
O2i—Cd1—O1	106.1	(2)	C15B—C14B—C13B	108.3	(15)
O2i—Cd1—C1i	27.41	(19)	C15B—C14B—H14B	125.8	
O2—Cd1—C1i	131.8	(3)	C13B—C14B—H14B	125.8	
O2i—Cd1—O3Biii	119.1	(3)	O4B—C24B—C21B	118.7	(13)
O2—Cd1—O3Biii	84.0	(3)	O3B—C24B—O4B	125.2	(15)
O2—Cd1—O3Bii	119.1	(3)	O3B—C24B—C21B	116.1	(11)
O2i—Cd1—O3Bii	84.0	(3)	C23B—C22B—H22B	120.7	
O1i—Cd1—O1	98.3	(3)	C21B—C22B—C23B	118.7	(14)
O1i—Cd1—C1i	27.15	(19)	C21B—C22B—H22B	120.7	
O1—Cd1—C1i	105.5	(3)	C19B—C20B—C21B	120.1	(12)
O1—Cd1—O3Biii	96.2	(3)	C19B—C20B—H20B	119.9	
O1i—Cd1—O3Biii	165.3	(3)	C21B—C20B—H20B	119.9	
O1i—Cd1—O3Bii	96.2	(3)	C12ix—C17B—C18B	117.1	(13)
O1—Cd1—O3Bii	165.3	(3)	C16B—C17B—C12ix	128.9	(17)
O3Biii—Cd1—C1i	144.2	(3)	C16B—C17B—C18B	113.9	(16)
O3Bii—Cd1—C1i	88.5	(3)	C24A—O3A—Cd2	138.2	(16)
O3Bii—Cd1—O3Biii	69.3	(6)	C13A—N2A—C16A	96	(4)

O4Aii—Cd1—O2	113.9	(6)	N2A—C13A—C8	113	(5)
O4Aiii—Cd1—O2	82.2	(6)	N2A—C13A—C14A	122	(5)
O4Aii—Cd1—O1	166.5	(6)	C14A—C13A—C8	125	(4)
O4Aiii—Cd1—O1	77.6	(6)	C22A—C21A—C24A	120	(2)
O2iv—Cd2—O2v	81.4	(3)	C20A—C21A—C22A	117	(2)
O2v—Cd2—O3Aviii	155.2	(6)	C20A—C21A—C24A	123	(2)
O2iv—Cd2—O3A	155.2	(6)	C13A—C14A—H14A	127.8	
O2iv—Cd2—O3Aviii	78.2	(5)	C13A—C14A—C15A	104	(4)
O2v—Cd2—O3A	78.2	(5)	C15A—C14A—H14A	127.8	
O4Bvi—Cd2—O2iv	106.2	(2)	C18A—C19A—H19A	118.8	
O4Bvii—Cd2—O2iv	76.8	(3)	C20A—C19A—H19A	118.8	
O4Bvi—Cd2—O2v	76.8	(3)	C20A—C19A—C18A	122	(3)
O4Bvii—Cd2—O2v	106.2	(2)	C21A—C22A—H22A	120.8	
O4Bvi—Cd2—O4Bvii	176.2	(4)	C23A—C22A—C21A	118	(3)
O4Bvi—Cd2—O3Aviii	95.5	(5)	C23A—C22A—H22A	120.8	
O4Bvii—Cd2—O3Aviii	82.8	(5)	C14A—C15A—H15A	126.8	
O3Aviii—Cd2—O3A	124.8	(11)	C16A—C15A—C14A	106	(4)
Cd1—O2—Cd2iii	105.7	(2)	C16A—C15A—H15A	126.8	
C1—O2—Cd1	92.5	(4)	C12ix—C17A—C18A	120	(3)
C1—O2—Cd2iii	149.9	(5)	C12ix—C17A—C16A	117	(3)
C1—O1—Cd1	92.4	(5)	C16A—C17A—C18A	122	(4)
C12—N1—H1	125.7		C22A—C23A—H23A	116.2	
C12—N1—C9	108.7	(7)	C22A—C23A—C18A	128	(3)
C9—N1—H1	125.7		C18A—C23A—H23A	116.2	
N1—C12—C11	108.4	(7)	C19A—C18A—C17A	123	(3)
N1—C12—C17Bix	123.2	(10)	C23A—C18A—C19A	114	(3)
C11—C12—C17Bix	128.1	(11)	C23A—C18A—C17A	123	(3)
C17Aix—C12—N1	134.7	(18)	C15A—C16A—N2A	110	(4)
C17Aix—C12—C11	116.3	(17)	C15A—C16A—C17A	122	(5)
C11—C10—H10	126.1		C17A—C16A—N2A	128	(4)
C11—C10—C9	107.8	(8)	O4A—C24A—O3A	128	(2)
C9—C10—H10	126.1		O4A—C24A—C21A	115	(2)
C12—C11—H11	126.7		O3A—C24A—C21A	117	(2)
C10—C11—C12	106.6	(9)	C21A—C20A—H20A	119.6	
C10—C11—H11	126.7		C19A—C20A—C21A	121	(3)
N1—C9—C10	108.5	(8)	C19A—C20A—H20A	119.6	
N1—C9—C8	126.6	(8)	C2B—C3B—H3B	120.0	
C8—C9—C10	124.8	(7)	C2B—C3B—C4B	120.0	
C9—C8—C13A	124	(2)	C4B—C3B—H3B	120.0	
C9—C8—C5B	120.2	(9)	C3B—C2B—C1	118.0	(5)
C9—C8—C5A	109.2	(18)	C7B—C2B—C1	121.8	(5)
C13B—C8—C9	126.2	(12)	C7B—C2B—C3B	120.0	
O2—C1—C2B	120.8	(6)	C2B—C7B—H7B	120.0	
O2—C1—C2A	115.8	(16)	C2B—C7B—C6B	120.0	
O1—C1—O2	120.2	(7)	C6B—C7B—H7B	120.0	
O1—C1—C2B	119.0	(7)	C7B—C6B—H6B	120.0	
O1—C1—C2A	123.6	(15)	C5B—C6B—C7B	120.0	
C24B—O4B—Cd2x	137.0	(8)	C5B—C6B—H6B	120.0	
C24B—O3B—Cd1v	98.4	(9)	C6B—C5B—C8	121.8	(6)
C16B—N2B—C13B	113.2	(17)	C6B—C5B—C4B	120.0	
N2B—C16B—C15B	106.0	(19)	C4B—C5B—C8	118.1	(6)
N2B—C16B—C17B	125	(2)	C3B—C4B—H4B	120.0	
C17B—C16B—C15B	129	(2)	C5B—C4B—C3B	120.0	
C18B—C19B—H19B	119.7		C5B—C4B—H4B	120.0	
C20B—C19B—H19B	119.7		C6A—C5A—C8	117	(2)
C20B—C19B—C18B	120.7	(14)	C6A—C5A—C4A	120.0	
C16B—C15B—H15B	125.4		C4A—C5A—C8	123	(2)
C14B—C15B—C16B	109.2	(18)	C5A—C6A—H6A	120.0	
C14B—C15B—H15B	125.4		C7A—C6A—C5A	120.0	
C18B—C23B—H23B	119.2		C7A—C6A—H6A	120.0	
C18B—C23B—C22B	121.7	(14)	C6A—C7A—H7A	120.0	
C22B—C23B—H23B	119.2		C2A—C7A—C6A	120.0	
C22B—C21B—C24B	120.5	(13)	C2A—C7A—H7A	120.0	
C22B—C21B—C20B	118.2	(13)	C7A—C2A—C1	116	(2)
C20B—C21B—C24B	121.3	(11)	C7A—C2A—C3A	120.0	
C8—C13B—N2B	132	(2)	C3A—C2A—C1	124	(2)
C8—C13B—C14B	125.2	(17)	C2A—C3A—H3A	120.0	
N2B—C13B—C14B	103.1	(18)	C4A—C3A—C2A	120.0	
C19B—C18B—C17B	118.2	(14)	C4A—C3A—H3A	120.0	
			C5A—C4A—H4A	120.0	
			C3A—C4A—C5A	120.0	

Symmetry codes: (i) $-x+3, y, -z+3/2$; (ii) $-x+3/2, y+1/2, -z+3/2$; (iii) $x+3/2, y+1/2, z$; (iv) $-x+1/2, y-1/2, -z+3/2$; (v) $x-3/2, y-1/2, z$; (vi) $-x, y, -z+3/2$; (vii) $x-1, y, z$; (viii) $-x-1, y, -z+3/2$; (ix) $-x+1/2, -y+3/2, -z+1$; (x) $x+1, y, z$.

Topology analysis of compound 1

The topology of compound **1** was performed with the ToposPro program package and the TTD collection of periodic network topologies.¹ If we carry out simplification by standard procedure, we obtain a 4,4,8-c net, which is a new trinodal network (Fig. S1(d)). It will be named *nnu3* and will be added to TTD-collection in the following update. The point symbol of the net is $(4^4.6^2)_2(4^8.6^4.8^{16})$. Both types of 4-coordinated nodes correspond to Cd atoms (Fig. S1(a) and Fig. S1(b)), the 8-coordinated nodes are the centers of mass of 5,10,15,20-*tetrakis*(4-carboxylatophenyl) porphyrin ligands (Fig. S1(c)).

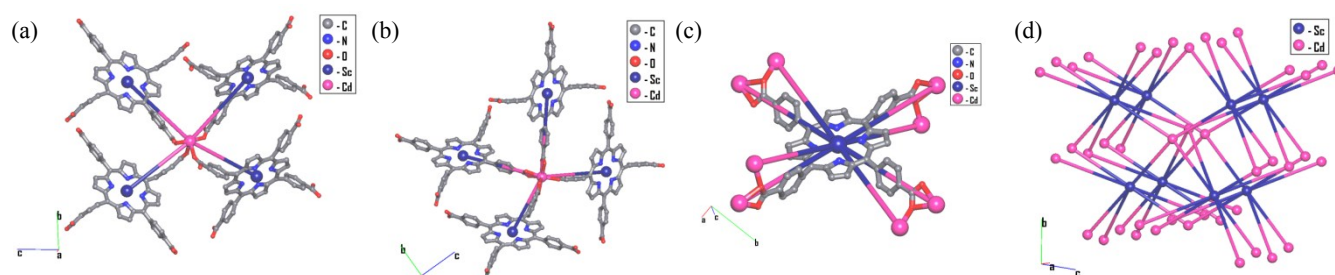


Fig. S1 4,4,8-c underlying net (*nnu3*) of compound 1.

(a) the coordination mode of one sort of Cd atoms. (b) the coordination mode of second sort of Cd atoms. (c) the O⁴⁴ coordination mode of a 5,10,15,20-*tetrakis*(4-Carboxylatophenyl)porphyrin ligand. (d) the overall net.

Another method of analysis of compound **1** is the cluster simplification procedure. Compound **1** contains one-periodic secondary building units, they are called rod SBUs (Fig. S2(a)).² The composition of infinite rod is $[\text{CdC}_2\text{O}_4]_n$. The Cd atoms form two types of polyhedra: trigonotetrahedron (8 O atoms) and tetrahedron (4 O atoms), which share the opposite edges (Fig. S2(b)). Each rod SBU is connected to eight other rods by four ligands as shown in Fig. S2(c). If we project atoms on the (100) plane (Fig. S2(c)), we can conclude, that there are two kinds of nonequivalent 4-coordinated nodes: the projections of the middle lines of the rods and the centers of the mass of the ligands. As a result, structure has tetragonal rod packing.

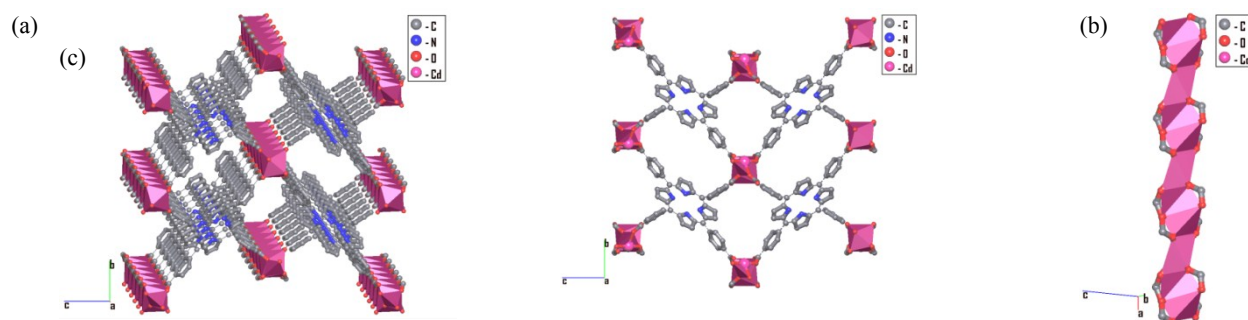


Fig. S2 The rod packing structure of compound 1

(a) the parallel rod SBUs, (b) the projection of parallel rod SBUs on the (100) plane, (c) the $[\text{CdC}_2\text{O}_4]_n$ rod constructed by edge-sharing polyhedra.

Compound **1** can be simplified in a third way by the cluster simplification method. This method proposes to consider some valence bonds, in particular, C1-C2, C5-C8, C13-C14 and C17-C20 as intercluster (Fig. S3(a)). Additionally, we manually changed all valence bonds of Cd2 atoms to intercluster for isolation of the CdC_4O_8 clusters, which contain only Cd1 atoms (Fig. S3(b)). Now, there are no parallel infinite valence bonded CdC_2O_4 clusters and we can provide the second step of the classical cluster simplification procedure: all valence-bonded groups should be contracted to their centers of mass. The resulting underlying net is 2-nodal 4,6-coordinated with point symbol $(4^2.6^4)(4^2.6^8.7^3.8^2)$. Topological type is 4,6T156. The coordination modes of the central atoms, ligands and the underlying net itself are showed in Fig. S3(c)-(f).

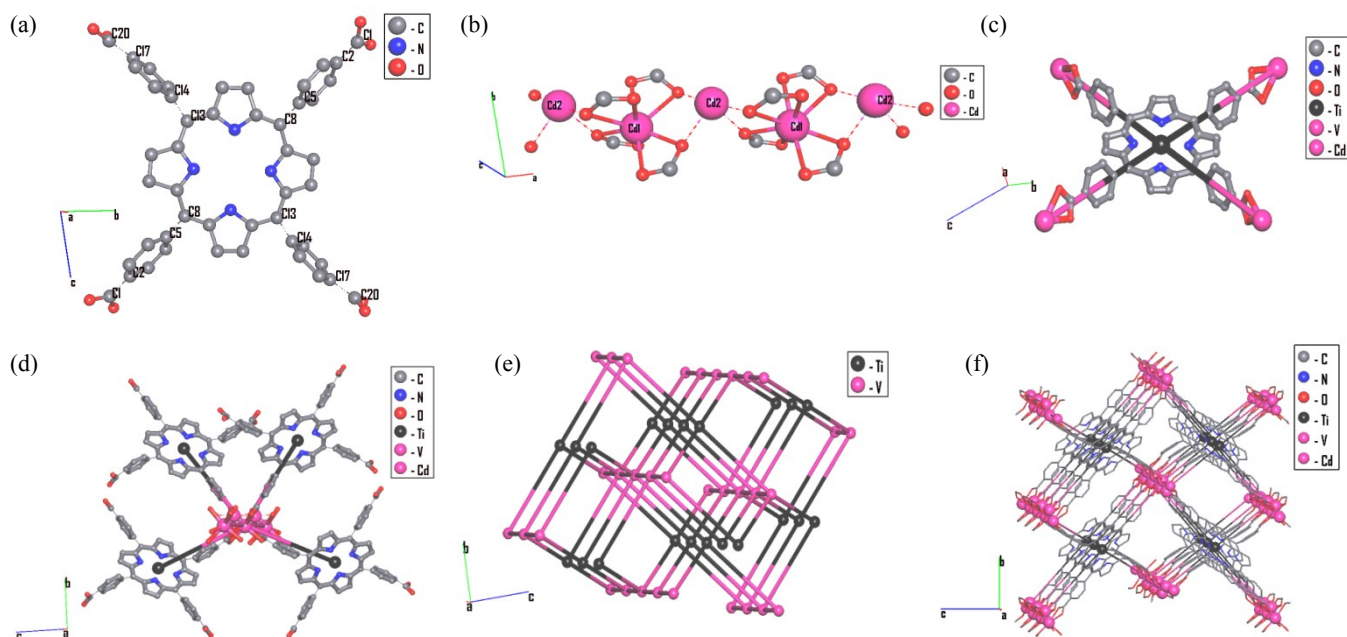


Fig. S3 The 2-nodal 4,6-coordinated 4,6T156 topology of compound 1.

(a) 5,10,15,20-*tetrakis*(4-Carboxylatophenyl)porphyrin) ligand after cluster simplification. (b) Separated clusters with the composition CdC_4O_8 (Cd1) by Cd2 atoms. (c) The coordination mode of a 5,10,15,20-*tetrakis*(4-carboxylatophenyl)porphyrin) ligand. Black balls is the center of mass of the ligand; magenta balls are centers of mass of the CdC_4O_8 clusters (they coincide with Cd atoms). (d) the coordination mode of a Cd1 atom. (e) 4,6T156 net (f) the initial structure and the 4,6T156 net are combined.

The TTD collection contains only five records for 4,6T156 topological type. There is an isostructural series of four compounds, which are constructed by the same ligand (5,10,15,20-*tetrakis*(4-carboxylatophenyl)porphyrin)),³ the fifth compound contains a μ -4,4',4'',4'''-pyrene-1,3,6,8-tetrayltetrabenzoate ligand.⁴

IR spectra

We recorded the IR spectrum of H_6 TCPP, which is consistent with the reported spectrum.⁵ We also recorded the Raman spectrum of H_6 TCPP (Fig. S4(c)). The IR spectra of **1**-DMF, **1**(4:1)-4d-DMF, **1**(6:1)-4d-DMF and **1**(8:1)-4d-DMF (Fig. S4(a)) are all the same, showing a band at 1707 cm^{-1} which is too high to be assigned to a C=O stretching of DMF molecules ($1670\text{--}1690\text{ cm}^{-1}$). By comparing the IR spectrum of **1**(8:1)-4d-DMF with those of **1**-ex and H_6 TCPP in Fig. S4(c), we think this band is due to H_6 TCPP trapped between crystals or in the channels, which was not washed completely away by DMF solvent. In contrast, the solvent exchanged sample (**1**-ex) contains no H_6 TCPP and DMF molecules and should represent the IR spectrum of compound **1**. The IR peaks of H_6 TCPP at 3420 , 1695 , 1405 , and 1265 cm^{-1} (Fig. S4(c)) are assigned to the stretching vibrations of O-H, C=O, and C-O bonds of carboxylic acid groups according to literature.⁵⁻⁷ Consistently, the Raman spectrum of H_6 TCPP (Fig. S4(c)) shows no strong peaks in the range of those frequencies since these bonds are all very polar. The strong band at 1605 and the weak peak at 1560 cm^{-1} were assigned by others to C=C and C=N stretchings.⁵⁻⁷ The C=O distances are varied in a relatively large range according to the crystal structure of **1** (e.g. $1.2500(74)$, $1.26(2)$ and $1.29(2)\text{ \AA}$ in **1**). Thus it is possible there are two bands due to asymmetric stretching of CO_2^- . Since 1541 cm^{-1} is very strong, it should not be a C=C stretching band, we therefore assigned the strong bands at 1603 and 1541 cm^{-1} to asymmetric stretching of CO_2^- , and the strong peak at 1387 cm^{-1} to symmetric stretching of CO_2^- .

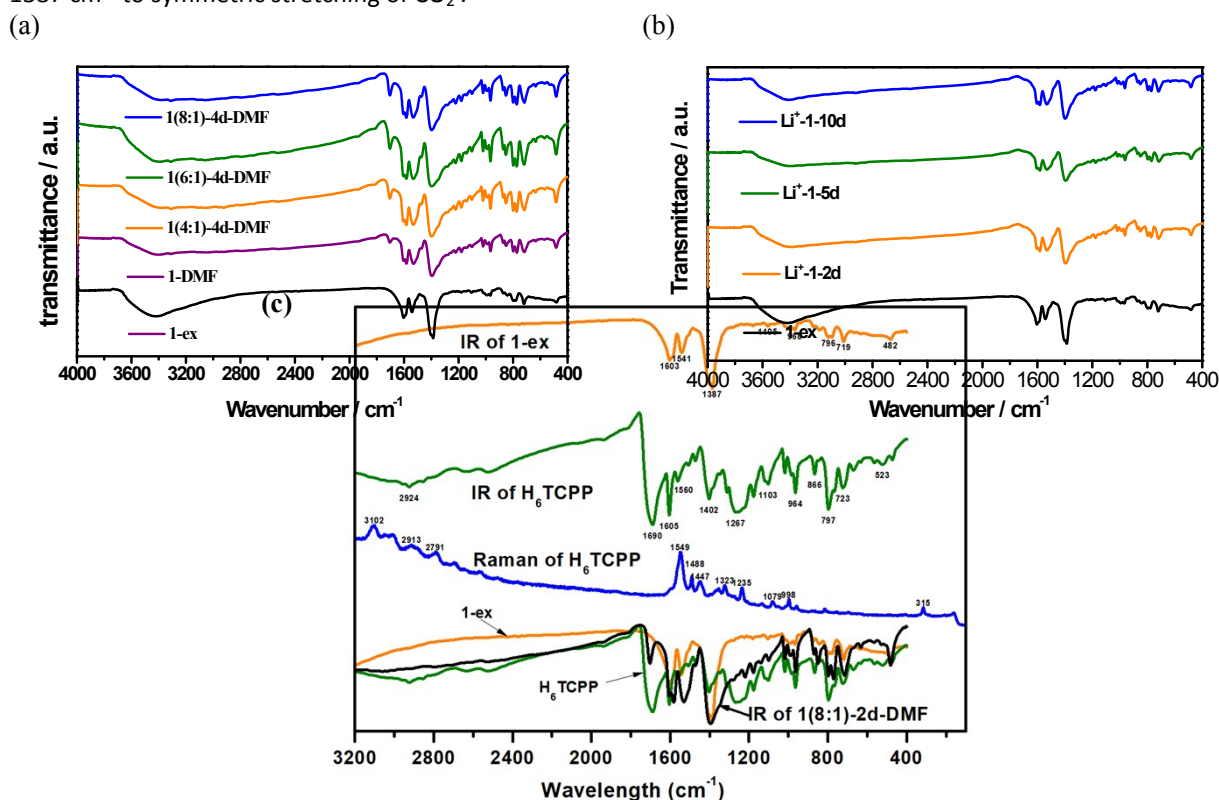
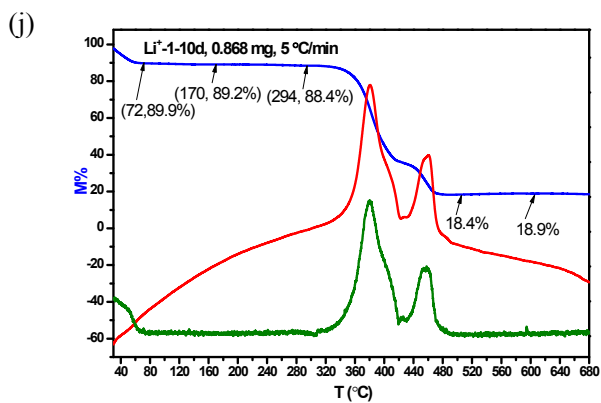
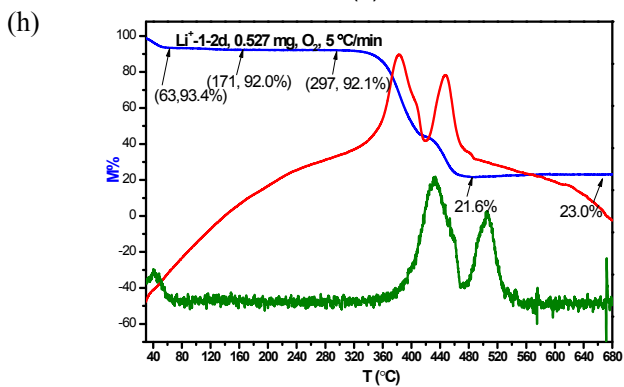
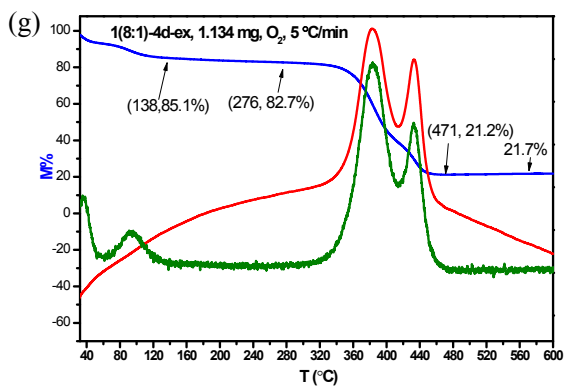
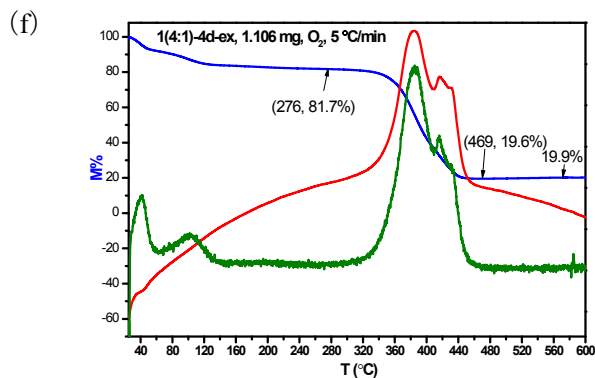
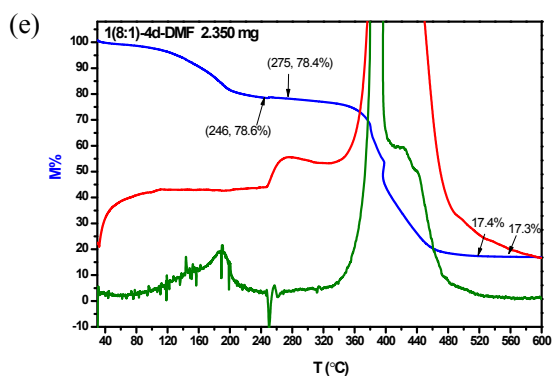
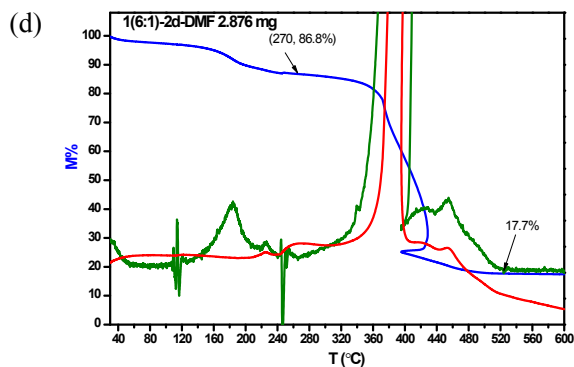
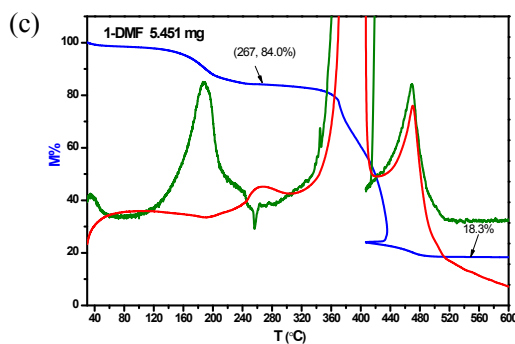
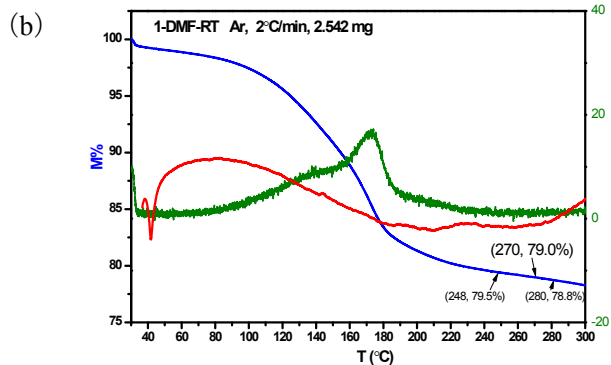
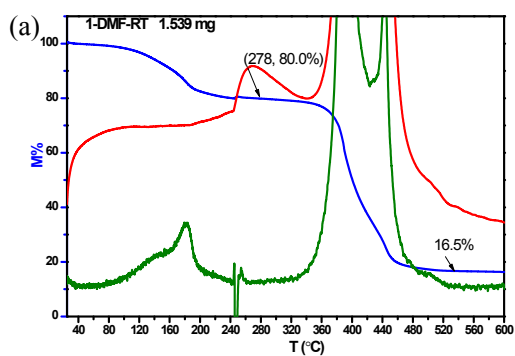


Fig. S4 IR spectra of **1**-DMF, **1**-ex, **1**(4:1)-4d-DMF, **1**(6:1)-4d-DMF, and **1**(8:1)-4d-DMF (a); IR spectra of Li^+ -1-2d, Li^+ -1-5d, and Li^+ -1-10d (b); IR and Raman spectra of H_6 TCPP compared with IR spectra of **1**-ex and **1**(8:1)-4d-DMF (c).



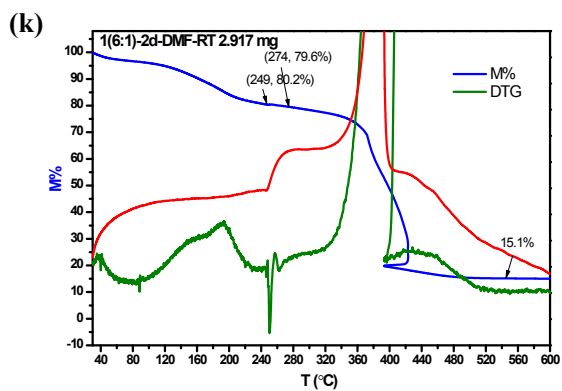


Fig. S5 TG (blue)/DTA(red)/DTG(green) of MOF 1 and its derived products.

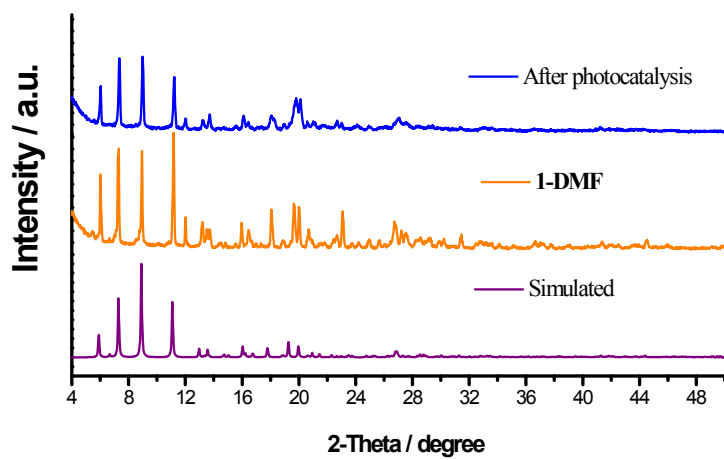


Fig. S6 PXRD spectrum of 1-DMF after two cycles of photocatalytic CO₂ reduction.

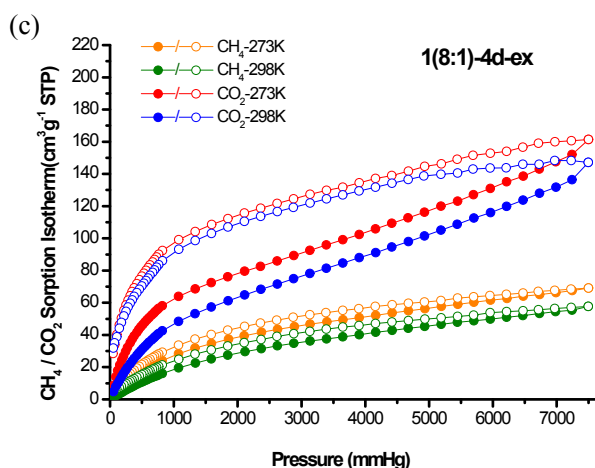
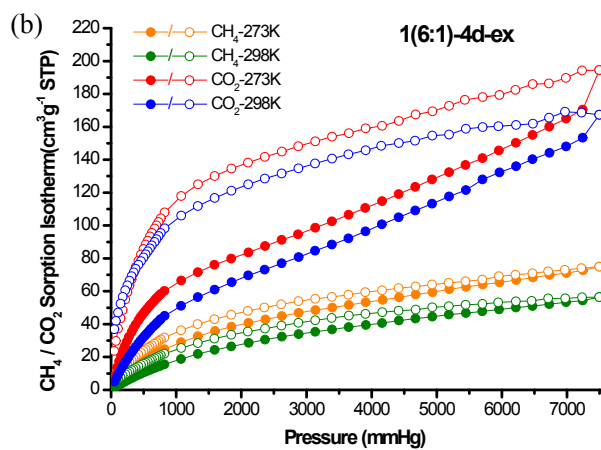
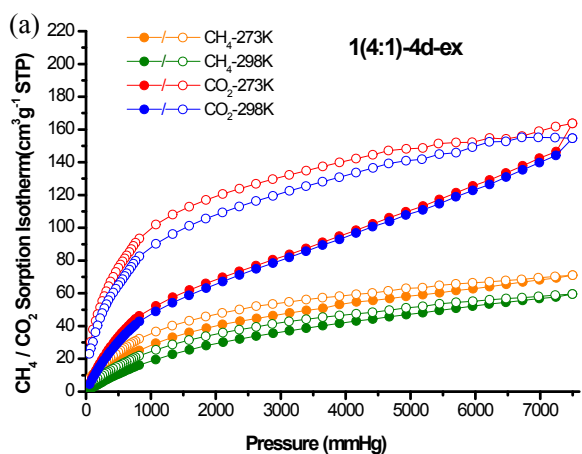


Fig. S7 CO₂ (273 and 298 K) and CH₄ (273 and 298 K) adsorption/desorption isotherms of 1(4:1)-4d-ex (a), 1(6:1)-4d-ex (b), and 1(8:1)-4d-ex (c).

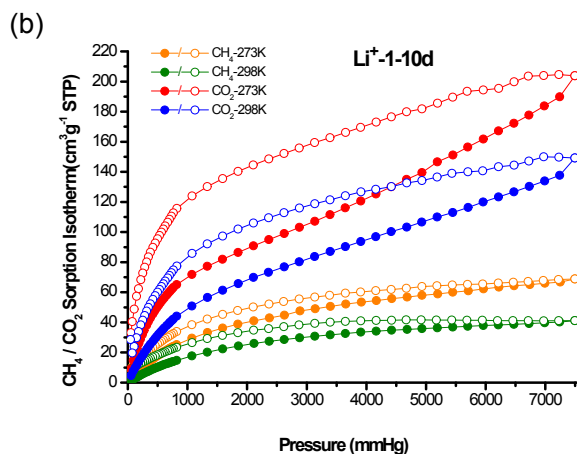
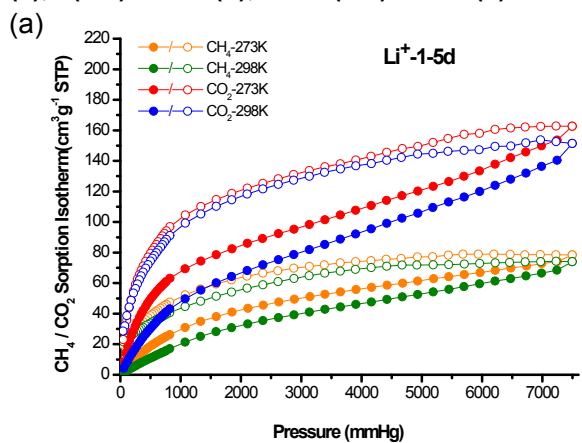


Fig. S8 CO₂ (273 and 298 K) and CH₄ (273 and 298 K) adsorption/desorption isotherms of Li⁺-1-5d (a) and Li⁺-1-10d (b).

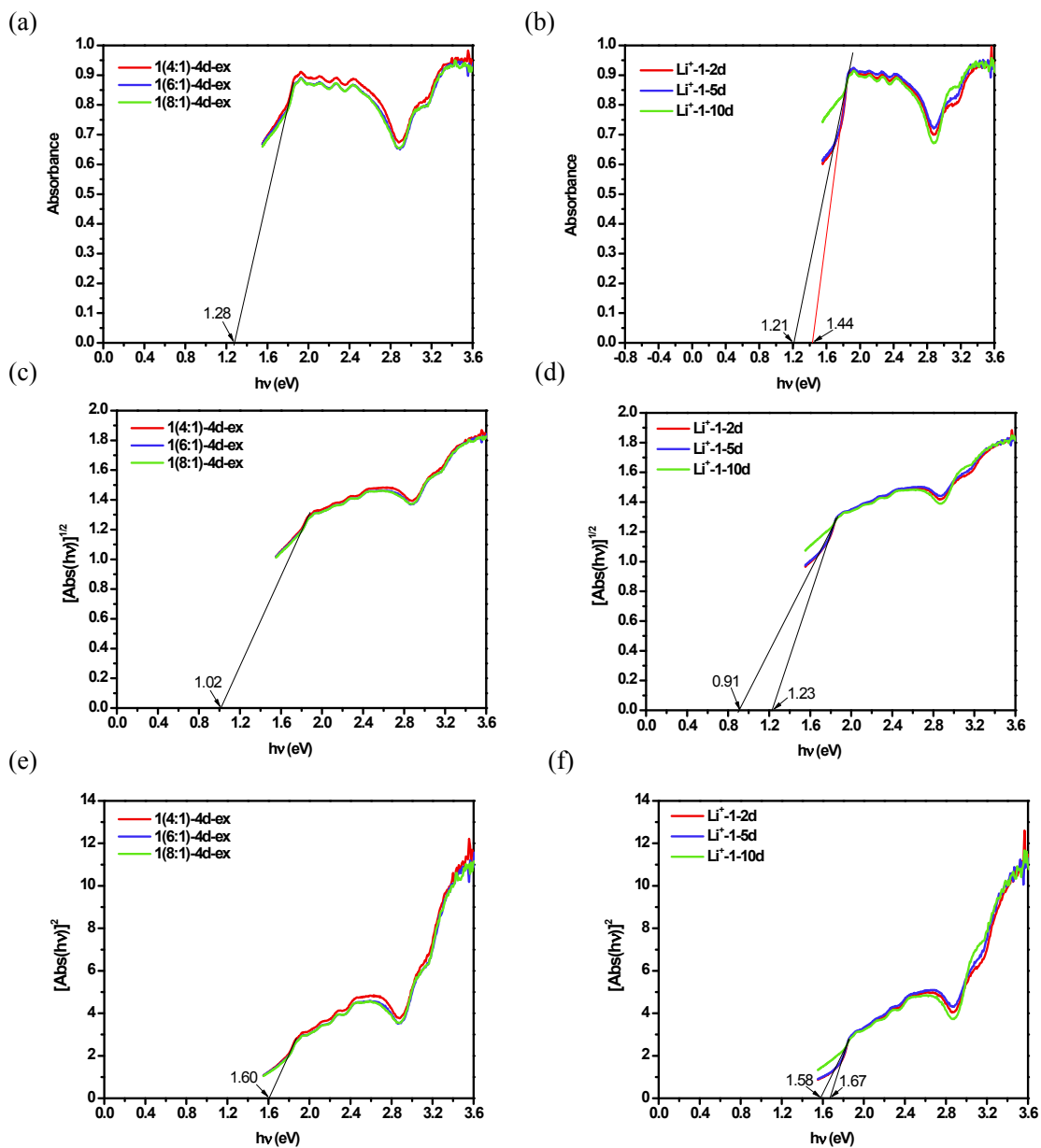


Fig. S9 Band gaps of 1(4:1)-4d-ex, 1(6:1)-4d-ex, 1(8:1)-4d-ex, Li^+ -1-2d, Li^+ -1-5d, and Li^+ -1-10d determined by plots of $(\text{abs or } [\text{abs}(h\nu)]^{1/2} \text{ or } [\text{abs}(h\nu)]^2$ versus $h\nu$.

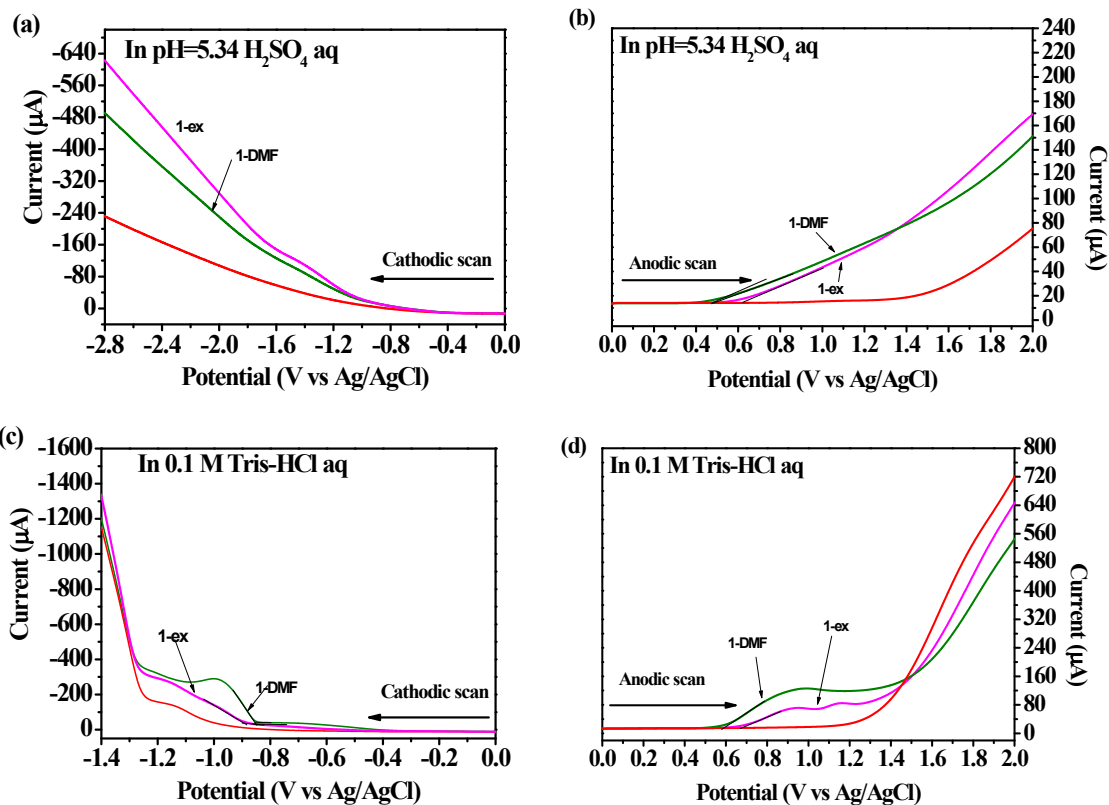
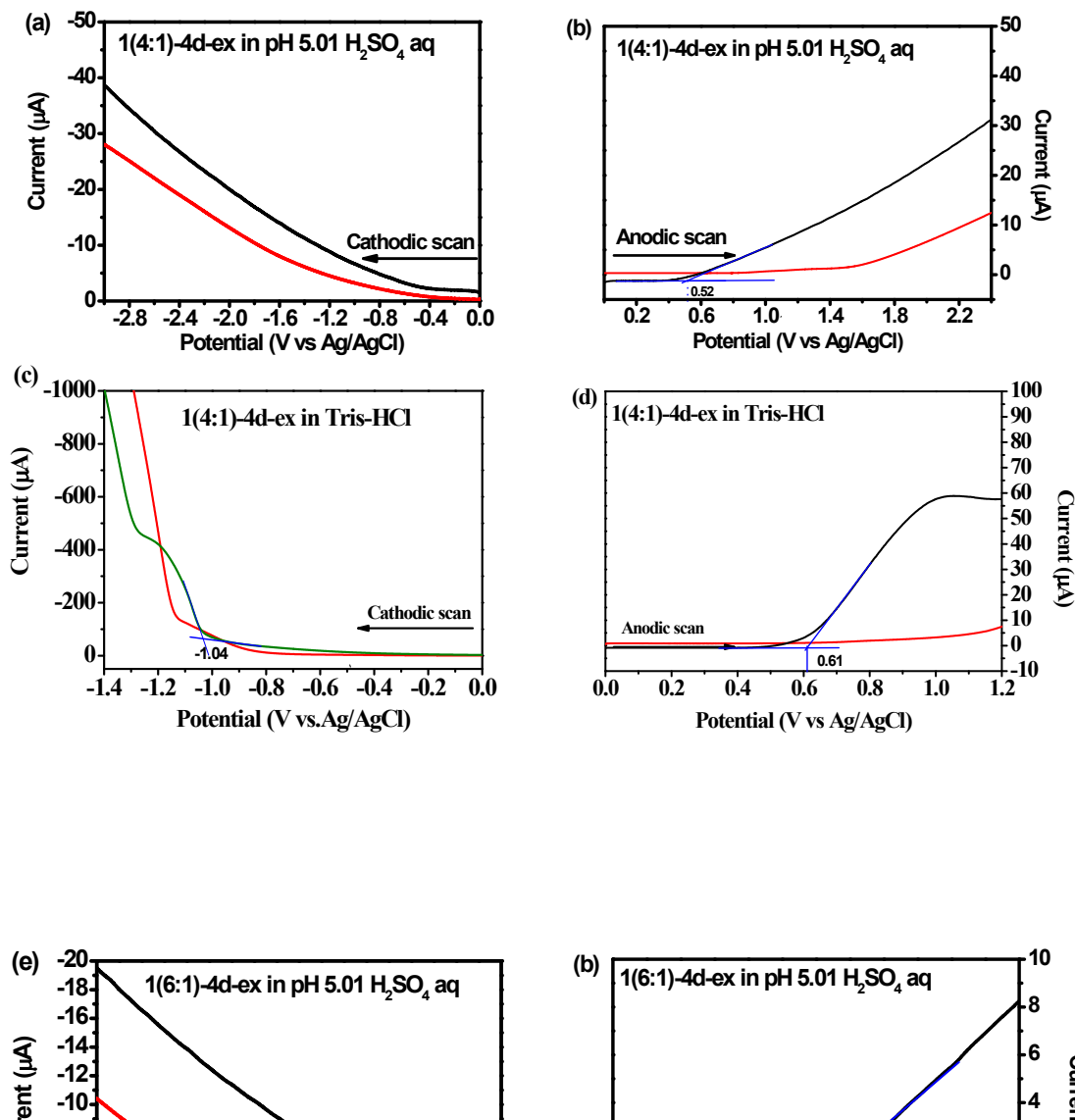


Fig. S10 Cathodic and anodic linear potential scans for determining the positions of the CB and VB edges of 1-DMF, and 1-ex using pH=5.34 H₂SO₄ aqueous solution or the **Tris-HCl buffered saline solution (0.1 mol L⁻¹, pH 7.4)**. The red curves are the currents of the electrolytes using the unmodified ITO electrodes.



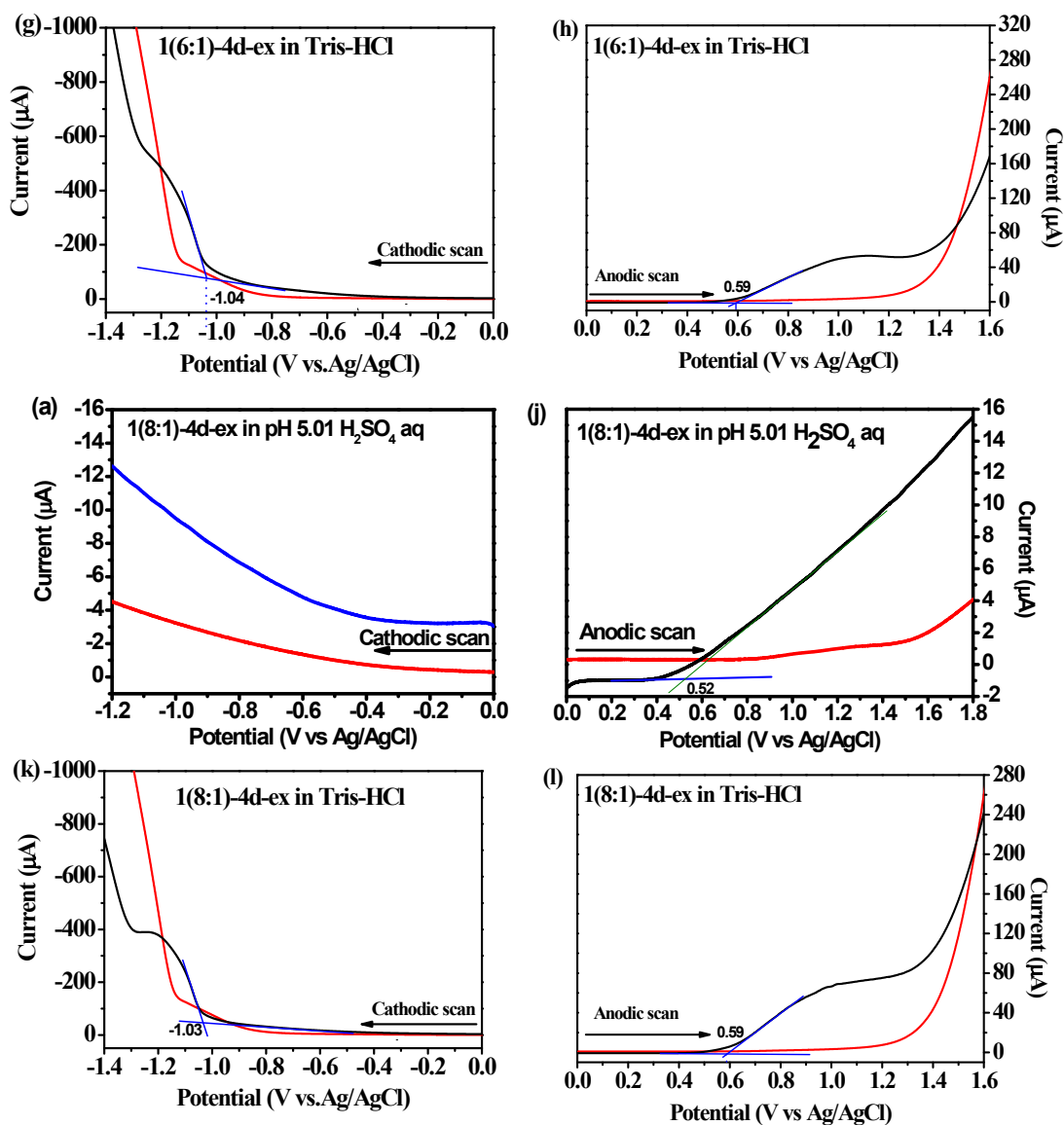
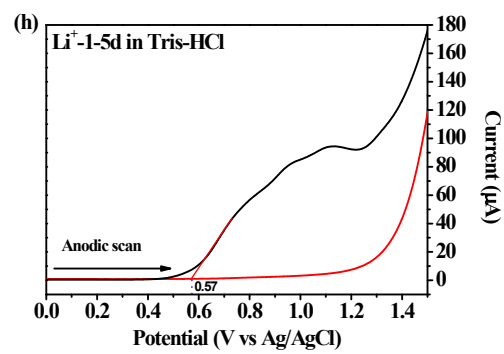
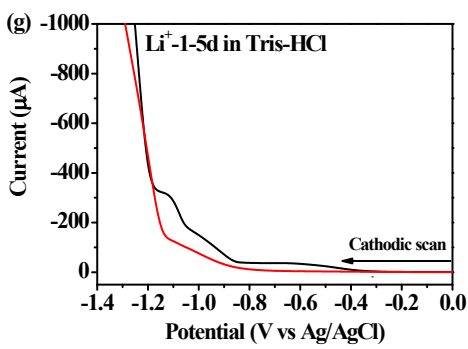
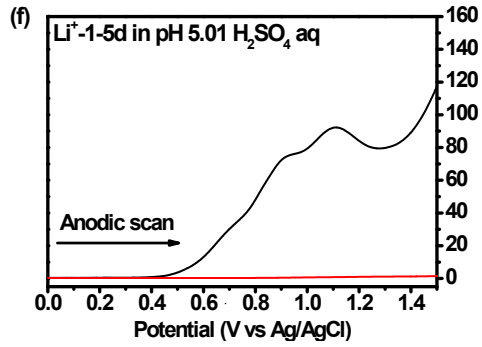
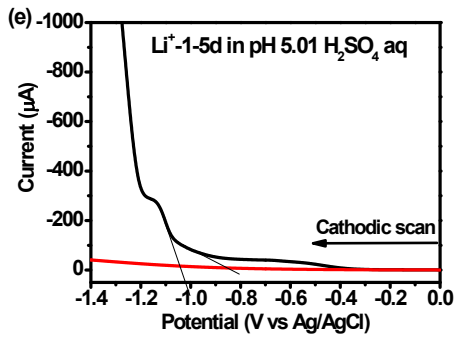
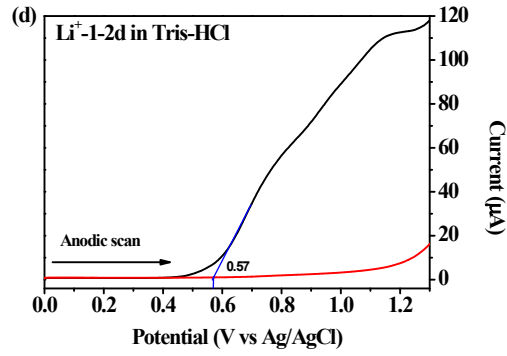
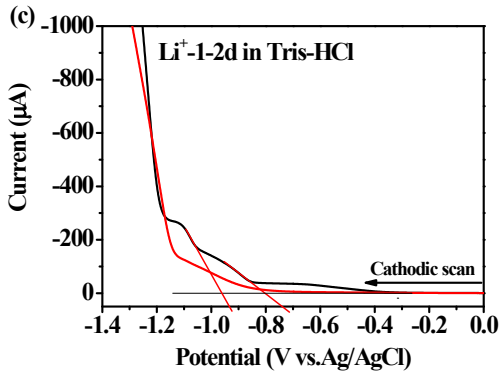
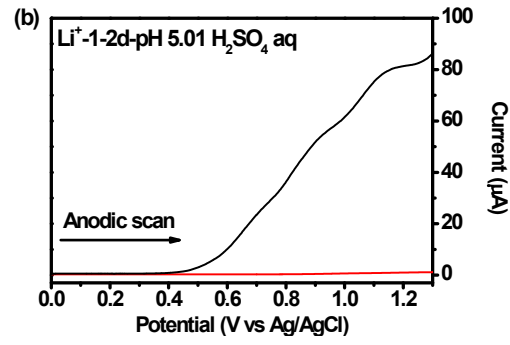
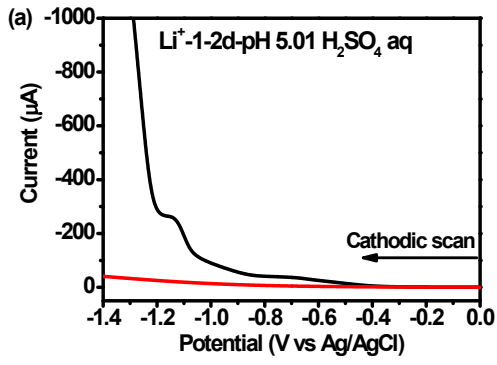


Fig. S11 Cathodic and anodic linear potential scans for determining the positions of the CB and VB edges of 1(4:1)-4d-ex ((a)-(d)), 1(6:1)-4d-ex ((e)-(h)) and 1(8:1)-4d-ex ((i)-(l)) using two different electrolytes (the pH 5.01 H₂SO₄ aqueous solution or the Tris-HCl buffered saline solution (0.1 mol·L⁻¹, pH 7.4)). The red curves are the currents of the electrolytes using the unmodified ITO electrodes.



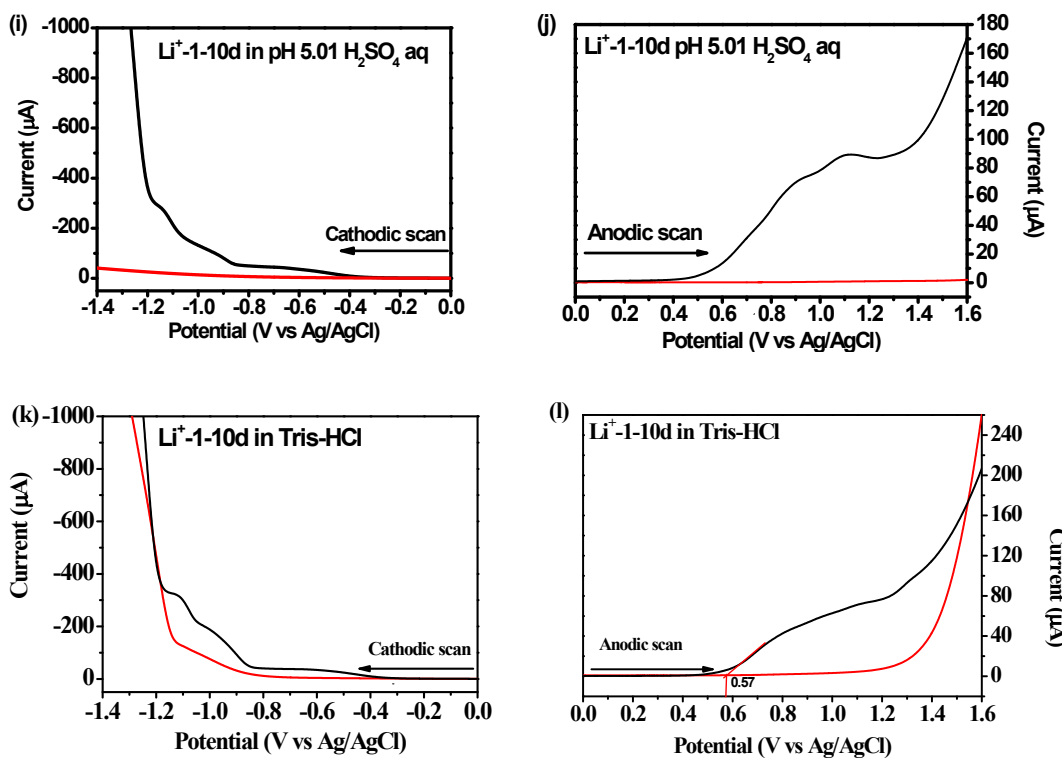


Fig. S12 Cathodic and anodic linear potential scans for determining the positions of the CB and VB edges of **Li⁺-1-2d** ((a)-(d)), **Li⁺-1-5d** ((e)-(h)) and **Li⁺-1-10d** ((i)-(l)) using two different electrolytes (the pH 5.01 H₂SO₄ aqueous solution or the **Tris-HCl buffered saline solution (0.1 mol L⁻¹, pH 7.4)**). The red curves are the currents of the electrolytes using the unmodified ITO electrodes.

References

1. V. A. Blatov, A. P. Shevchenko and D. M. Proserpio, *Cryst. Growth Des.*, 2014, **14**, 3576–3586.
2. N. L. Rosi, J. Kim, M. Eddaoudi, B. Chen, M. O’Keeffe and O. M. Yaghi, *J. Am. Chem. Soc.*, 2005, **127**, 1504-1518.
3. M. H. Xie, X. L. Yang and C. D. Wu, *Chemical Communications*, 2011, **47**, 5521-5523.
4. R.-J. Li, M. Li, X.-P. Zhou, D. Li and M. O’Keeffe, *Chemical Communications*, 2014, **50**, 4047-4049.
5. R. Rahimi, S. Saadati and E. H. Fard, *Environmental Progress & Sustainable Energy*, 2015, **34**, 1341-1348.
6. Q. Wang, W. M. Campbell, E. E. Bonfantani, K. W. Jolley, D. L. Officer, P. J. Walsh, K. Gordon, R. Humphry-Baker, M. K. Nazeeruddin and M. Gratzel, *Journal of Physical Chemistry B*, 2005, **109**, 15397-15409.
7. G. Granados-Oliveros, E. A. Paez-Mozo, F. Martinez Ortega, C. Ferronato and J.-M. Chovelon, *Applied Catalysis B-Environmental*, 2009, **89**, 448-454.